

Electronic Supplementary Information (ESI)

Nano vs. bulk rutile TiO₂:N,F in Z-scheme overall water splitting
under visible light

*Akinobu Miyoshi,^{1,2} Kosaku Kato,³ Toshiyuki Yokoi,⁴ Jan J. Wiesfeld,⁵ Kiyotaka Nakajima,⁵ Akira
Yamakata,³ and Kazuhiko Maeda^{1,*}*

¹ Department of Chemistry, School of Science, Tokyo Institute of Technology, 2-12-1-NE-2
Ookayama, Meguro-ku, Tokyo 152-8550, Japan

² Japan Society for the Promotion of Science, Kojimachi Business Center Building, 5-3-1
Kojimachi, Chiyoda-ku, Tokyo 102-0083, Japan

³ Graduate School of Engineering, Toyota Technological Institute, 2-12-1 Hisakata, Tempaku,
Nagoya 468-8511, Japan

⁴ Nanospace Catalysis Unit, Institute of Innovative Research, Tokyo Institute of Technology,
4259-S2-5, Nagatsuta, Midori-ku, Yokohama 226-8503, Japan

⁵ Institute for Catalysis, Hokkaido University, Kita 21 Nishi 10, Kita-ku, Sapporo 001-0021, Japan

*To whom correspondence should be addressed.

maedak@chem.titech.ac.jp

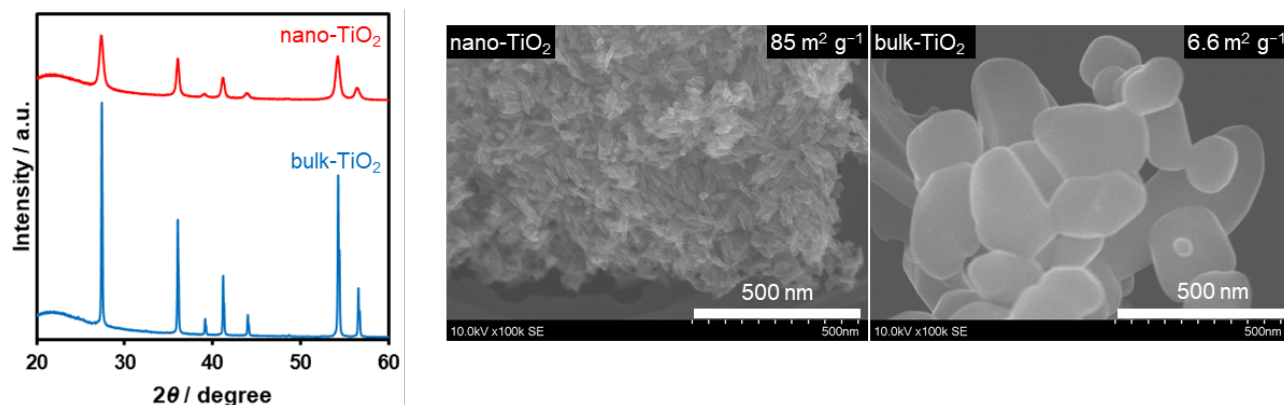


Fig. S1. XRD patterns and SEM images of the rutile TiO₂ precursors used for synthesizing TiO₂:N,F.

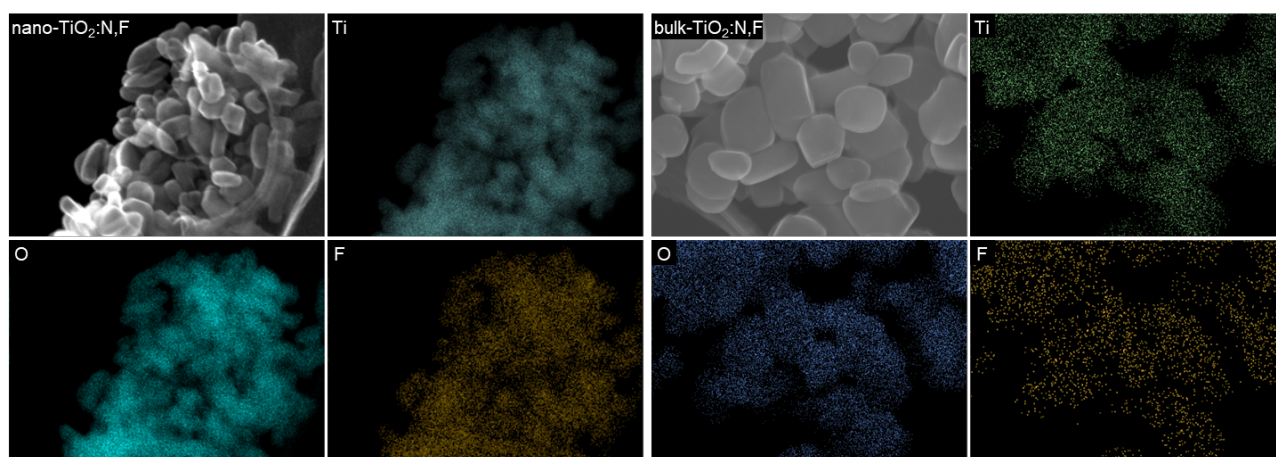


Fig. S2. EDX elemental mapping of nano- and bulk-TiO₂:N,F synthesized under optimized conditions. Although the signals of nitrogen coincide with those of titanium and the distribution cannot be visualized, nitrogen was detected by combustion elemental analysis (Table S1 and S2).

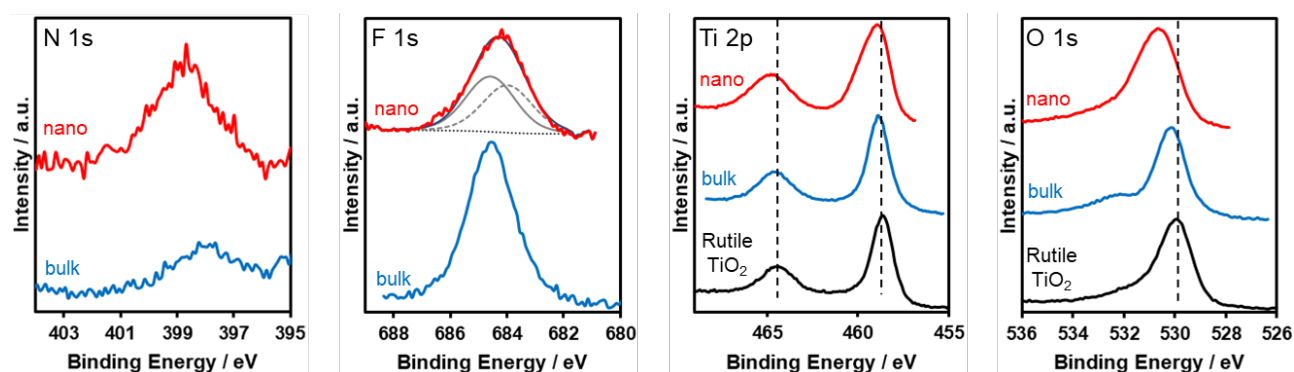


Fig. S3. X-ray photoelectron spectra of nano- and bulk-TiO₂:N,F synthesized under optimized conditions. The grey lines and the black solid line in the F 1s spectra of the nano material are deconvoluted peaks and a fitting curve derived from the deconvoluted peaks, respectively. The black broken line is a baseline used for fitting.

Additional discussion on the XPS results

Electronic states of constituent elements of nano- and bulk-TiO₂:N,F were investigated by XPS. For F 1s peak, bulk-TiO₂:N,F showed a peak at 684.6 eV. On the other hand, nano-TiO₂:N,F exhibited a rather broader peak, which suggests that there are at least two peaks. Deconvolution was conducted, assuming that there is a peak at same position as the bulk material. This resulted in two peaks centred at 684.6 and 684.0 eV, with a full-width-half-maxima similar to that of the bulk material, indicative of the validity of the deconvolution. Zhao et al. proposed that a peak at 684.2 eV in F-doped anatase TiO₂ is attributed to surface adsorbed fluorine species.^{S1} Therefore, the 684.0 eV peak observed in the present work would be attributed to the surface adsorbed fluorine. It is known that fluorine doped at the oxygen site of anatase TiO₂ gives peaks at 685.4 and 687.9 eV, depending on the surrounding environment.^{S1} As the binding energy range of the doped fluorine is generally wide (depending on the structure), the peak at 684.6 eV may be associated with fluorine doped into the oxygen site of rutile TiO₂.

The incorporation of fluorine seems to have affected the electronic states of Ti and O. The Ti 2p and O 1s peaks of TiO₂:N,F were located at higher energies relative to pristine rutile TiO₂. This suggests that the high electronegativity of fluorine reduced the electron density around Ti and O atoms. Some literatures reported that the addition of fluorine into TiO₂ elongated the lifetime of excited electrons on Ti.^{S2-4} As Ti in nanomaterials have lower density of electrons than the bulk counterparts, the fluorine incorporation into TiO₂ may have played a role in making the lifetime of free or shallowly trapped electrons longer. This, indeed, does not contradict the results of transient absorption spectroscopy, as discussed in this work.

However, the assignment of N 1s peaks in N-doped TiO₂ has been under debate.^{S5} So, it was not possible to attribute the peaks observed in this work to specific nitrogen species. Yet, the N 1s peak of nano-TiO₂:N,F shifted to higher energy side than that of the bulk, similar to those observed in the Ti 2p and O 1s peaks. Except for this high binding energy shift in nano-TiO₂:N,F, all of the features for nano and bulk materials were similar. Therefore, it is likely that the doped nitrogen species giving rise to the visible light absorption observed in DRS (Fig. 1B) are similar in both materials.

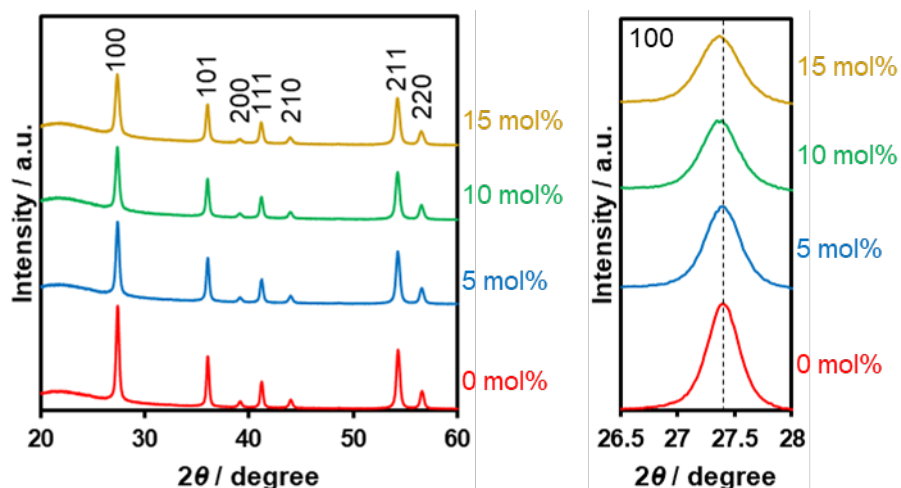


Fig. S4. XRD patterns of nano-TiO₂:N,F prepared by nitridation of a mixture of nano-TiO₂ and (NH₄)₂TiF₆ at various concentration of (NH₄)₂TiF₆. Nitridation condition: 673 K for 15 h under 30 mL min⁻¹ NH₃ flow.

Additional discussion on the XRD of results

Synthesis of nano-TiO₂:N,F was conducted using precursor mixtures with various concentrations of the fluorine source. The XRD patterns of the obtained materials shown in Fig. S4 indicated a peak shift toward lower diffraction angles. This is similar to the results obtained for similar consideration conducted for bulk-TiO₂:N,F in previous work.^{S6} From this result along with the results of EDS and XPS, doping of the anions into the TiO₂ lattice was strongly suggested.

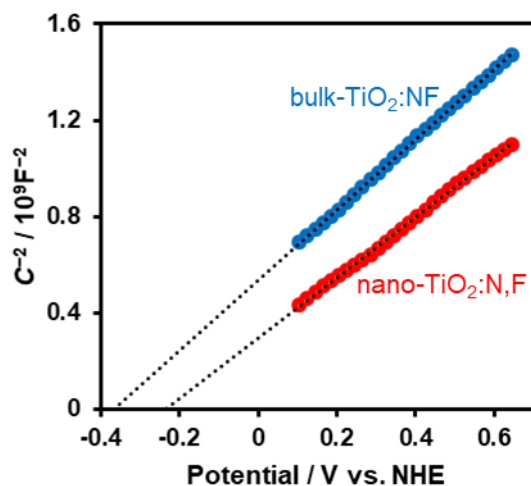


Fig. S5. Mott-Schottky plots of nano- and bulk-TiO₂:N,F synthesized under optimized conditions. Electrolyte: 0.1 M Na₂SO₄ (pH 6.0), frequency: 500 Hz.

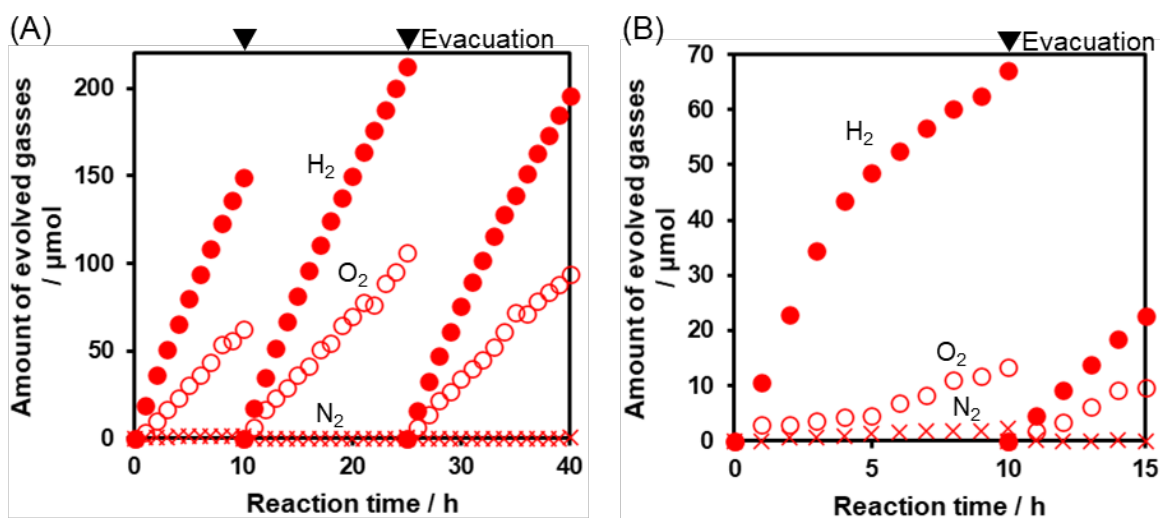


Fig. S6. Time courses of gas evolution from the visible-light Z-scheme water-splitting system constructed using (A) nano- and (B) bulk-TiO₂:N,F synthesized under optimized conditions. Reaction conditions: TiO₂:N,F, 50 mg; Ru/SrTiO₃:Rh, 25 mg; 0.5 mM Co(bpy)₃SO₄ aq. 140 mL. Light source: 300 W Xe lamp fitted with CM-1 mirror and an L42 cutoff filter ($\lambda > 420$ nm). The initial stage of the reaction included an induction period for O₂ evolution due likely to the absence of [Co(bpy)₃]³⁺ at this stage. The longer induction period of bulk-TiO₂:N,F is therefore considered to arise from lower reactivity of the material with [Co(bpy)₃]³⁺ compared to nano-TiO₂:N,F, as indicated by the result of transient absorption spectroscopy.

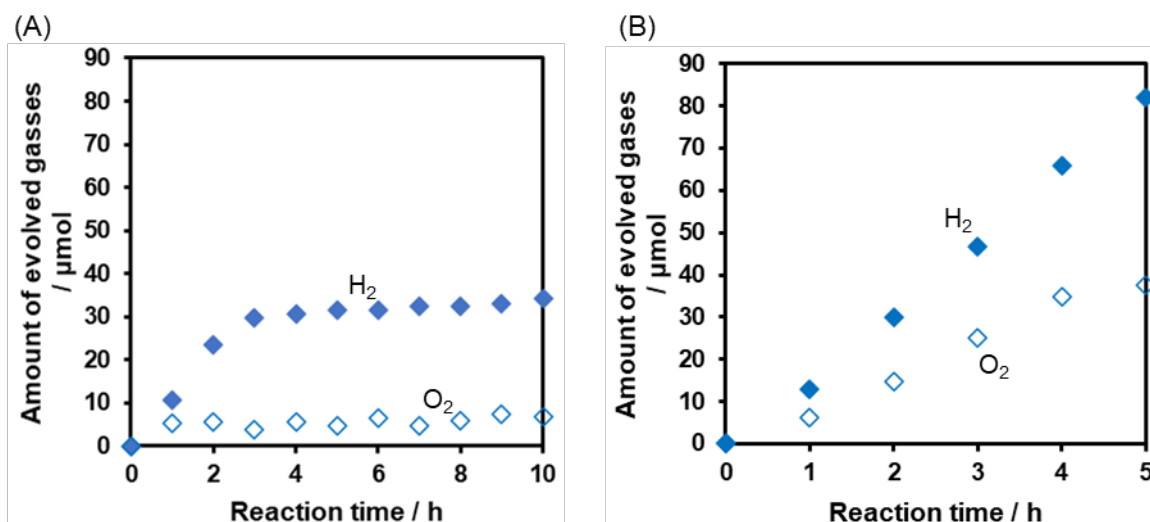


Fig. S7. Time courses of gas evolution from the visible-light Z-scheme water splitting systems constructed with different water oxidation photocatalysts: (A) nano-TiO₂ and (B) BiVO₄. Reaction conditions: O₂-evolution photocatalyst (nano-TiO₂ or BiVO₄), 50 mg; Ru/SrTiO₃:Rh, 25 mg; 0.5 mM Co(bpy)₃SO₄ aq. 140 mL. Light source: 300 W Xe lamp fitted with a CM-1 mirror and an L42 cutoff filter ($\lambda > 420$ nm). The origin of the O₂ evolution from nano-TiO₂ (in the panel A) is probably due to small residual absorption of TiO₂ that can respond to the incident light used.

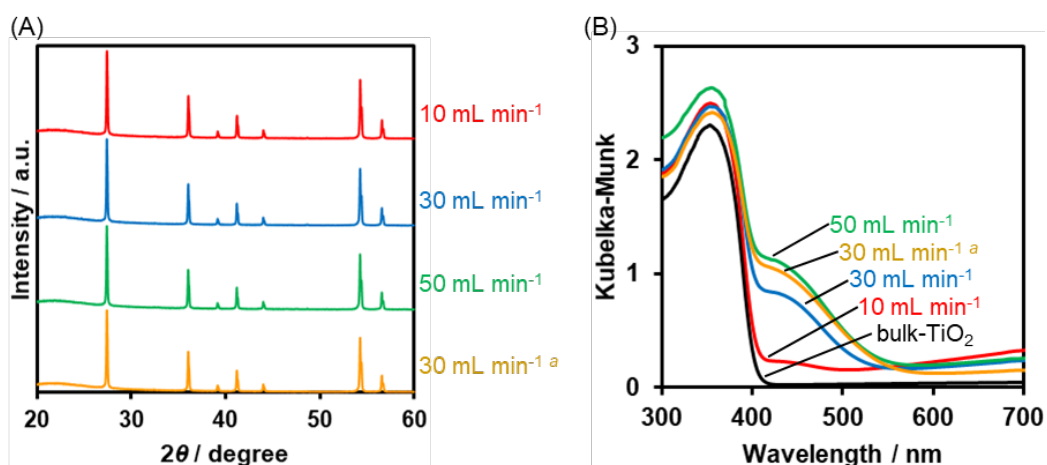


Fig. S8. (A) XRD patterns and (B) UV-vis DRS of bulk-TiO₂:N,F synthesized by nitridation at 773 K for 1 h under various NH₃ flow rates. ^aNitrided at 673 K for 15 h.

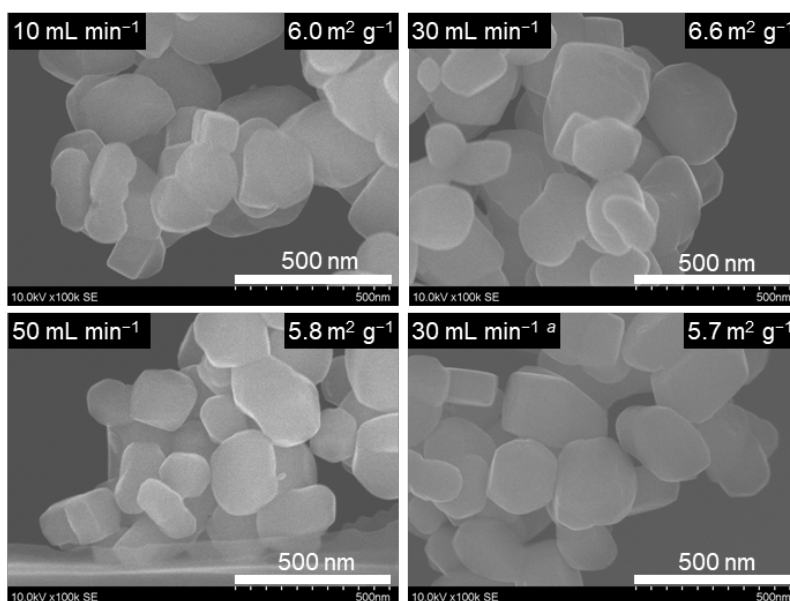


Fig. S9. SEM images and BET surface areas of bulk-TiO₂:N,F synthesized by nitridation at 773 K for 1 h under various NH₃ flow rates. ^aNitrided at 673 K for 15 h.

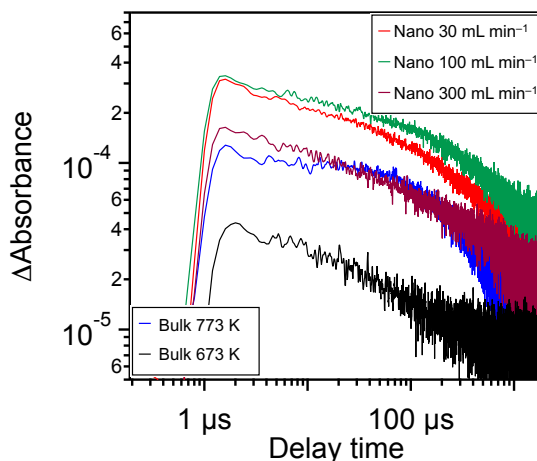


Fig. S10. Time profiles of differential absorbance at 2000 cm⁻¹ for nano- and bulk-TiO₂:N,F prepared under different conditions. Excitation wavelength: 420 nm (under a N₂ atmosphere).

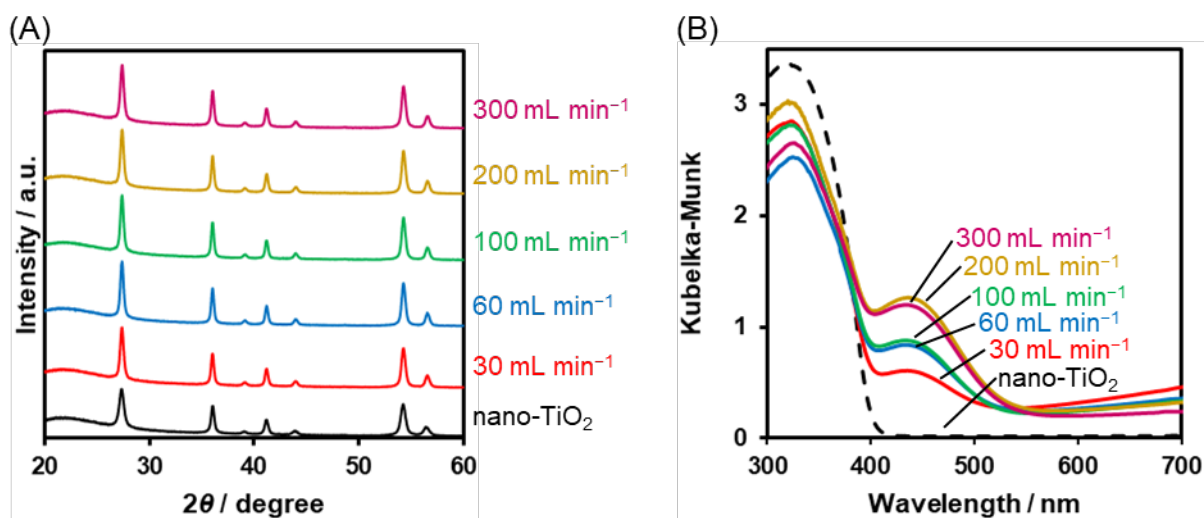


Fig. S11. (A) XRD patterns and (B) UV-vis DRS of nano-TiO₂:N,F synthesized by nitridation at 673 K for 15 h under various NH₃ flow rates.

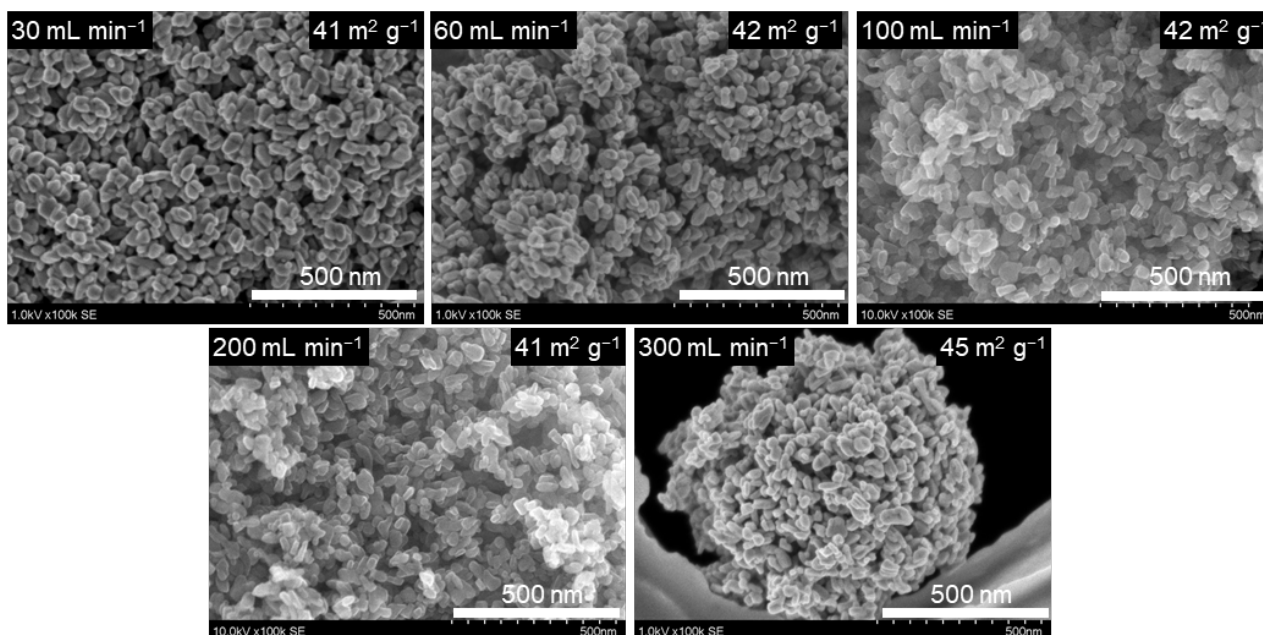


Fig. S12. SEM images and BET surface areas of nano-TiO₂:N,F synthesized by nitridation at 673 K for 15 h under various NH₃ flow rates.

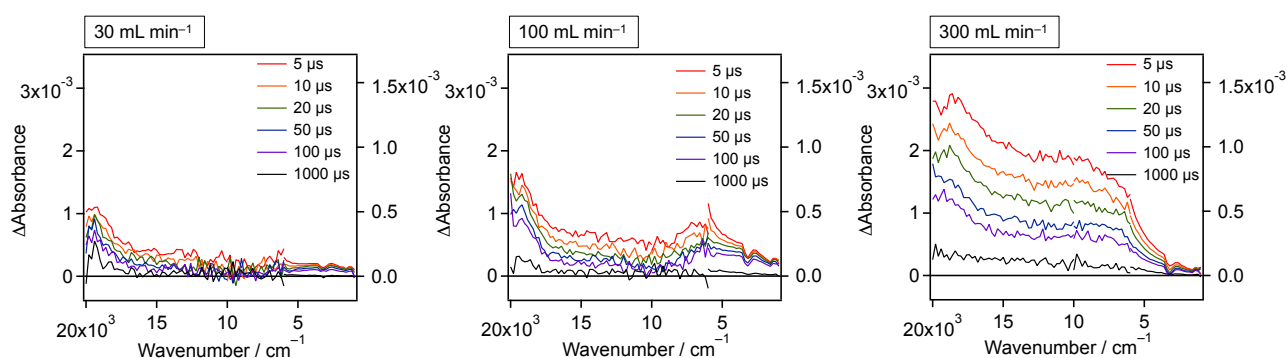


Fig. S13. Transient absorption spectra of nano-TiO₂:N,F prepared by nitridation at 673 K for 15 h under various NH₃ flow rates. The spectra were recorded under excitation with 420 nm laser pulses under a N₂ atmosphere. Transmittance and reflectance were measured in the wavenumber regions below and above 6000 cm⁻¹, respectively.

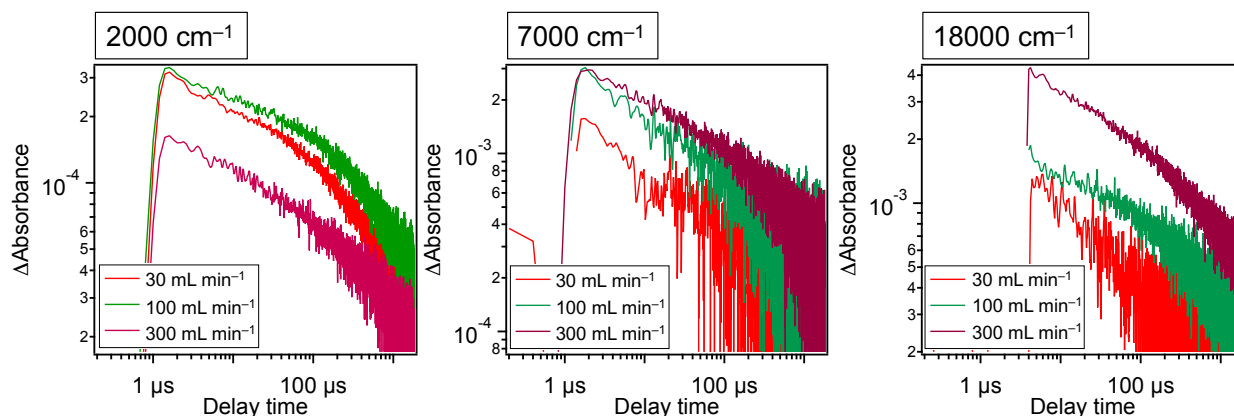


Fig. S14. Time profiles of differential absorbance at 2000, 7000 and 18000 cm⁻¹ for nano-TiO₂:N,F prepared under various NH₃ flow rates. Excitation wavelength: 420 nm (under a N₂ atmosphere).

Electronic Supplementary Information (ESI)

Table S1. Nitrogen and fluorine concentrations in bulk-TiO₂:N,F prepared by nitridation at 773 K for 1 h under various NH₃ flow rates and steady-state gas evolution rates of visible-light Z-scheme water splitting systems constructed using the same materials

Entry	NH ₃ flow rate / mL min ⁻¹	Atomic concentrations / wt%		Evolution rates ^a / μmol h ⁻¹	
		N	F	H ₂	O ₂
1	10	n.d.	0.71	3.8	1.5
2	30	0.15	0.95	4.5	2.2
3	50	0.35	0.63	3.5	1.7
4 ^b	30	0.38	0.90	1.7	0.8

^aReaction conditions: TiO₂:N,F (50 mg) and Ru/SrTiO₃:Rh (25 mg) dispersed in 140 mL of 0.5 mM [Co(bpy)₃]SO₄ aq. Light source: 300 W Xe lamp fitted with CM-1 mirror and L42 cutoff filter ($\lambda > 420$ nm). ^bNitrided at 673 K for 15 h.

Table S2. Nitrogen and fluorine concentrations in nano-TiO₂:N,F prepared by nitridation at 673 K for 15 h under various NH₃ flow rates and steady-state gas evolution rates of visible-light Z-scheme water splitting systems constructed using the same materials

Entry	NH ₃ flow rate / mL min ⁻¹	Atomic concentrations / wt%		Evolution rates ^a / μmol h ⁻¹	
		N	F	H ₂	O ₂
1	30	0.41	1.32	10.8	5.0
2	60	0.42	1.34	13.6	5.7
3	100	0.46	1.77	15.5 ± 1.9	7.7 ± 1.0
4	200	0.55	1.77	15.6	7.7
5	300	0.54	1.01	13.0	6.3

^aReaction conditions: TiO₂:N,F (50 mg) and Ru/SrTiO₃:Rh (25 mg) dispersed in 140 mL of 0.5 mM [Co(bpy)₃]SO₄ aq. Light source: 300 W Xe lamp fitted with CM-1 mirror and L42 cutoff filter ($\lambda > 420$ nm).

References

- S1. Y. Wang, H. Zhang, P. Liu, T. Sun, Y. Li, H. Yang, X. Yao and H. Zhao *J. Mater. Chem. A*, 2013, **1**, 12948.
- S2. S. N. Subbarao, Y. H. Yun, R. Kershaw, K. Dwight and A. Wold, *Inorg. Chem.*, 1979, **18**, 488.
- S3. J. C. Yu, J. Yu, W. Ho, Z. Jiang and L. Zhang, *Chem. Mater.*, 2002, **14**, 3808.
- S4. M. V. Dozzi, C. D'Andrea, B. Ohtani, G. Valentini and E. Selli, *J. Phys. Chem. C*, 2013, **117**, 25586.
- S5. M. Pisarek, M. Krawczyk, M. Hołdyński and W. Lisowski, *ACS Omega*, 2020, **5**, 8647.
- S6. A. Miyoshi, J. J. M. Vequizo, S. Nishioka, Y. Kato, M. Yamamoto, S. Yamashita, T. Yokoi, A. Iwase, S. Nozawa, A. Yamakata, T. Yoshida, K. Kimoto, A. Kudo and K. Maeda, *Sustainable Energy Fuels*, 2018, **2**, 2025.